4.3 EVALUATION OF ENSEMBLE-BASED PROBABILISTIC WEATHER INFORMATION FOR AIR TRAFFIC MANAGEMENT

Matthias Steiner*, Richard E. Bateman, Dan L. Megenhardt, and James O. Pinto

NCAR Research Applications Laboratory (RAL), Boulder, CO

1. INTRODUCTION

Weather conditions can seriously impact aircraft operations, which places great importance on how weather-related information is collected, managed, disseminated, and utilized in the air traffic management (ATM) decision-making process. The primary role of weather information is to provide guidance where and when aircraft may fly safely. Weather forecasts have to be translated into information that is directly relevant to the aviation users and service providers. The uncertainty of weather forecasts has to be accounted for as well in the risk assessment and decision-making process. Moreover, the expected increase in air traffic flow requires largely automated, machine-to-machine communicating decision-making tools to effectively assist the human managing the airspace.

Weather forecasting increasingly relies on ensemble-based probabilistic predictions. This paper discusses a novel concept of creating probabilistic scenario forecasts that are tailored from an aviation perspective. A preliminary assessment of the value of such ensemble-based probabilistic forecasts is presented as well. The focus is primarily on convective storms; however, the new concept is applicable to other aviation weather hazards also. The presented approach may be useful for en route air traffic management, but we envision that it could also be adapted for a terminal area focus.

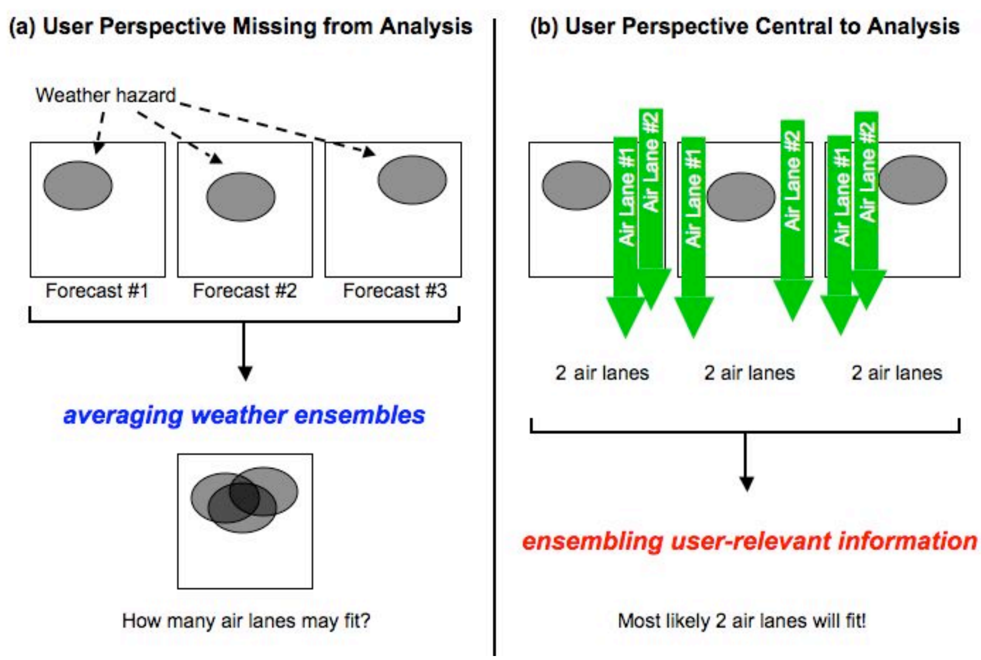

Figure 1. Contrasting concepts of aviation user involvement.

* *Corresponding author address*: Dr. Matthias Steiner, National Center for Atmospheric Research, Research Applications Laboratory, Boulder, Colorado 80307-3000; phone: 303/497-2720; email: msteiner@ucar.edu

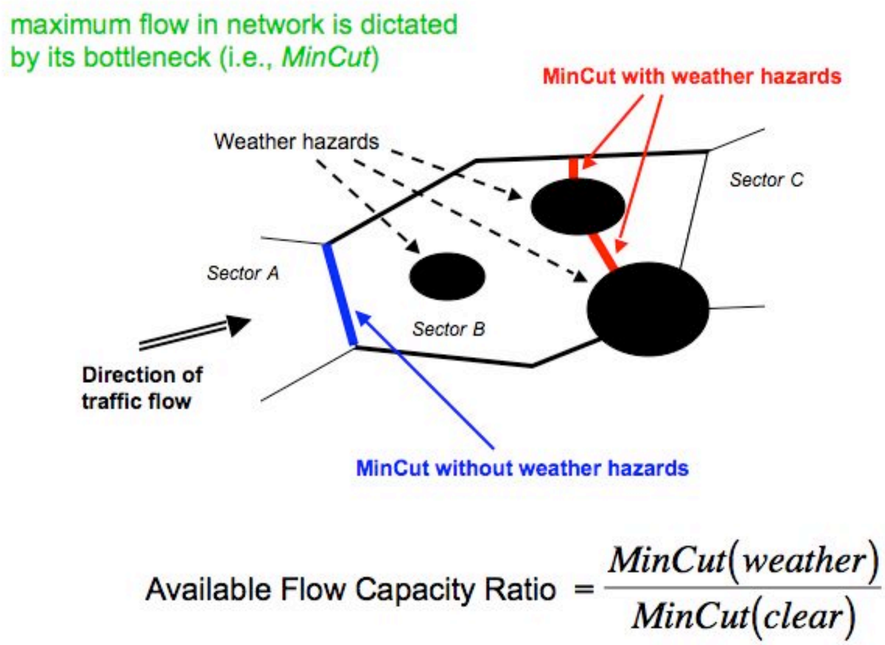

Figure 2. Translation of weather into ATM capacity impact based on utilizing MinCut theory.

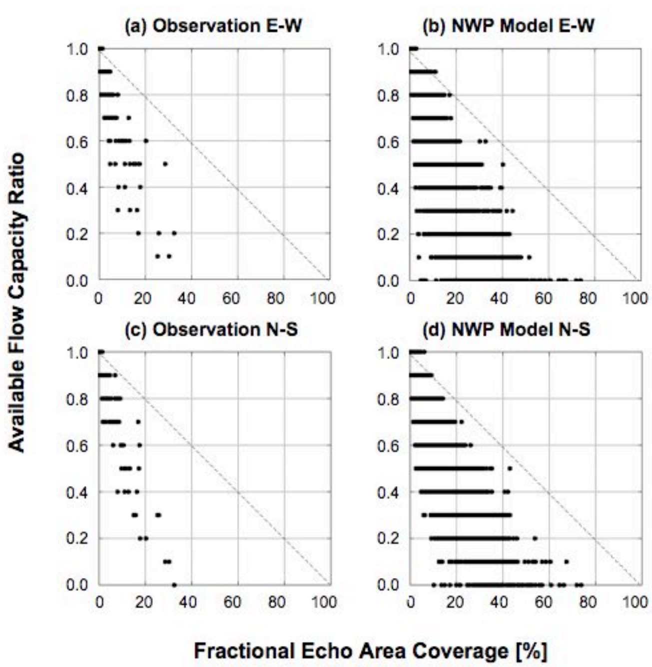

Figure 3. Relation between fractional echo area coverage and available flow capacity ratio.

2. AVIATION WEATHER FORECASTING

Steiner et al. (2008) presented a new concept of utilizing ensemble weather forecast output to create probabilistic predictions of aviation-relevant information. The central point of the advocated approach is to bring a user's perspective into the analysis of each ensemble forecast member and subsequently ensemble user-relevant information (Fig. 1). This is in stark contrast to generating a probabilistic weather forecast and then let the user figure out what to do with it.

Incorporation of the user application needs into the analysis essentially results in a translation of ensemble weather forecasts to probabilistic user-relevant information, as discussed next.

2.1 Translation of weather to ATM information

Aviation traffic flow managers are interested in how much traffic they may be able to pass through a given airspace at some point in the future. The available airspace capacity is a function of the amount of hazardous weather present as well as other factors, such as traffic controller workload and traffic demand. In addition, traffic constraints up- and downstream of a particular airspace may have an impact as well by limiting the overall flow.

From a network perspective, the maximum throughput is determined by its bottlenecks, which may be estimated based on the max-flow min-cut theorem (Mitchell et al. 2006; Krozel et al. 2007). For a given situation, the computed MinCut value depends on the spatial scale of the domain of interest, which is why a normalization of the MinCut is applied by dividing it with the corresponding MinCut value under no weather obstruction (Fig. 2). The resulting *available flow capacity ratio* (Song et al. 2007, 2008) represents a non-dimensional measure ranging between zero (i.e., unusable airspace without any capacity) and unity (fully usable airspace without weather constraints). Note, however, that airspaces may still have constraints based on controller workload, traffic demand, or flow constraints associated with up- and downstream air spaces, a fact that isn't consider in the present analyses. Thus, the results discussed in this paper are potential capacity estimates based on hazardous weather present in an airspace.

The available flow capacity ratio decreases sharply as weather hazards become more widespread. Figure 3 shows this relationship based on radar observations of convective weather and numerical weather prediction model output for both East-West (E-W) and North-South (N-S) traffic flows. The MinCut's are determined based on a Required Navigation Performance (RNP) of 4.

2.2 Ensemble forecasts for 27 – 29 June 2007

The 27 June 2007 date exemplifies a day when weather caused major delays across the northeastern United States (US). The New York area was particularly affected with average delays of several hours, but major delays were common to all major airports from the southeast to the northeast, and in the midwest. This massive, weather-related aviation impact was caused by a major outbreak of convective storms across the northeastern US that affected both en route traffic as well as arrival and departure routes of major airports.

This study utilized an operational ensemble model developed by the National Center for Atmospheric Research (NCAR) in support of the 4-dimensional weather (4DWX) forecasting effort at the Army Test and Evaluation Command (ATEC) ranges. Ensemble simulations were carried out with the Real-Time Four-Dimensional Data Assimilation (RT-FDDA) modeling system (Liu et al. 2006, 2007, 2008) using a setup of 28 ensemble members for two nested grids with 30 km and 10 km resolution. The results discussed here are based on the 10-km resolution domain that covers the northeastern US.

The domain covered by the 10-km ensemble model runs is shown in Fig. 4a together with the radar-observed and rain gauge-adjusted hourly precipitation accumulation ending at 21 UTC on 27 June 2007. The mean and standard deviation of the ensemble-based, 9-h forecast of the hourly precipitation accumulation valid at that time are illustrated in Figures 4b and 4c, respectively, while Figure 4d reveals the number of ensemble members exceeding a 2-mm hourly precipitation accumulation threshold. These ensemble model forecast summary plots indicate a widespread storm activity over the northeastern US; however, storm organization details are clearly lost in the averaging process.

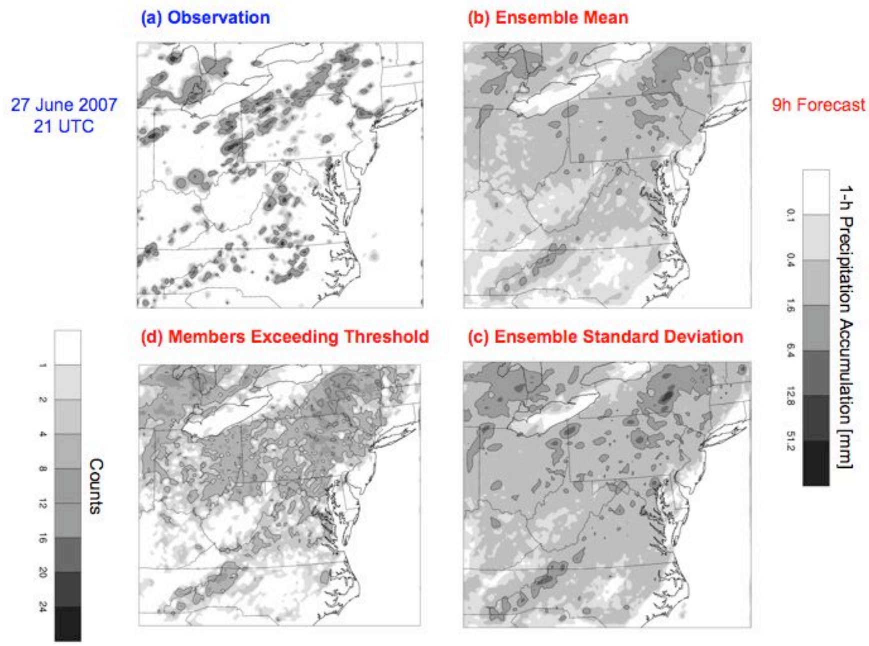

Figure 4. Observation and 9-h ensemble forecast information valid for 27 June 007 at 21 UTC.

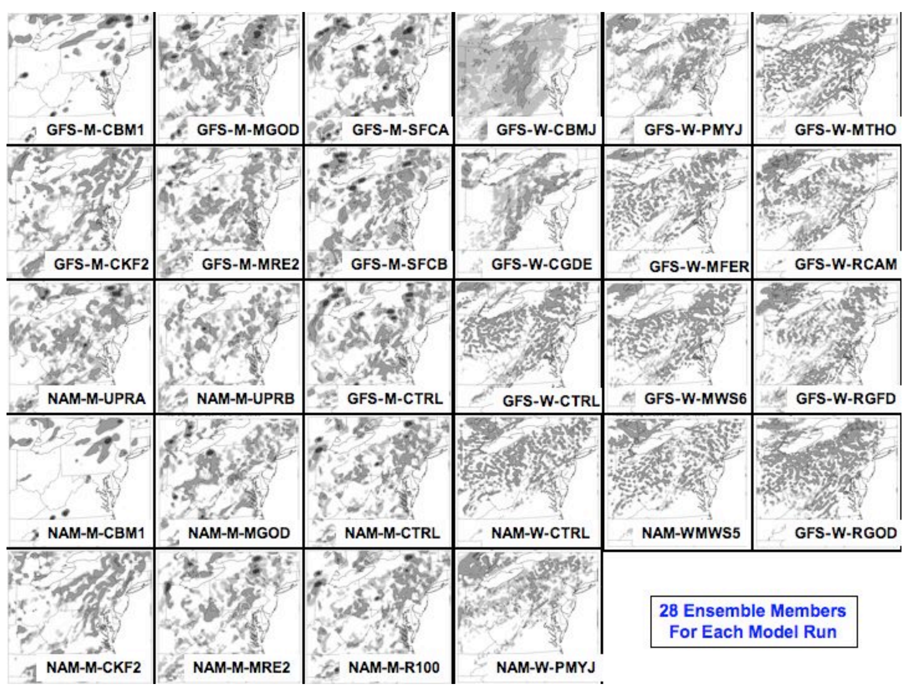

Figure 5. Individual ensemble members of the 9-h forecast valid for 27 June 2007 at 21 UTC. Details about the membership configuration are provided in Table 1.

The individual 28 members of that same 9-h ensemble precipitation forecast are presented in Figure 5. The 15 MM5-based forecasts (labeled "-M-") are shown on the left, 7 of which were initialized using the Global Forecast System (GFS) and 8 using the North American Model (NAM). The 13 WRF-based members (labeled "-W-") are shown on the right, with 10 members based on a GFS and 3 a NAM initialization, respectively. Figure 5 highlights a wide variety of possible weather outcomes, ranging from a few isolated intense storms (e.g., members GFS-M-CBM1 and NAM-M-CBM1) to widespread precipitation (e.g., member GFS-W-CBMJ), and much in between these two opposite outcomes.

The analysis steps of creating a probabilistic aviation user-relevant forecast are shown in Fig. 6. First, a grid of relevant shape and size (for simplicity we use a Cartesian grid here) gets overlaid on each ensemble forecast member (Fig. 6a). Second, for each gridbox the weather pattern is analyzed from a user perspective (utilizing the available flow capacity ratio as a measure) based on all ensemble members (Fig. 6b). Third, these ensemble-based gridbox values are rearranged and binned into a distribution of counts (Fig. 6c), which would be a probability density function (PDF) if properly calibrated. For illustration purposes, we utilize the cumulative distribution function (CDF) instead (Fig. 6d), which can be used to visualize the likelihood of exceeding a threshold. Figure 7, finally, shows the spatial likelihood of the available flow capacity ratio (RNP = 4) to drop below 0.7 (i.e., a 30% capacity reduction) based on a 9-h forecast and 50 km analysis grid. The warmer the colors in Fig. 7 (left panel) the higher the chance of losing capacity in E-W direction. The panel on the right in Fig. 7 shows the actual weather at forecast valid time.

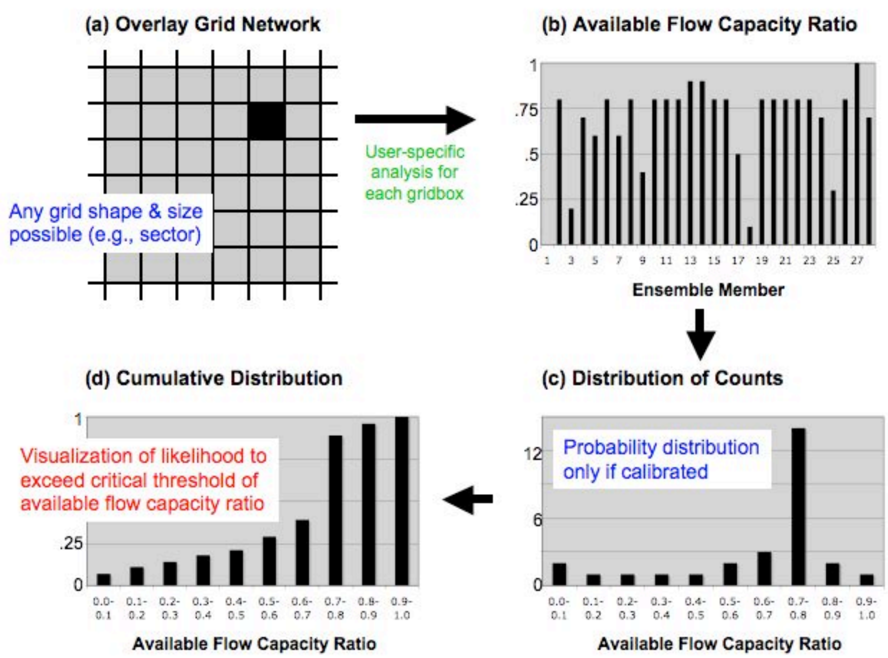

Figure 6. Analysis steps to create user-relevant probabilistic forecast information.

3. FORECAST EVALUATION

An objective assessment of the ensemble forecast system performance requires long-term comparisons of predictions and observations (e.g., Gneiting et al. 2007; Jones et al. 2007; Stensrud and Yussouf 2007). The amount of data collected and processed as part of this proof-of-concept analysis provides only limited insight to the overall performance of the ensemble forecast system. However, our analyses revealed some noteworthy results.

3.1 Weather focus

Figure 8, which is based on a single gridbox, shows that the performance of the 9-h ensemble forecast varies with time—for example, the center 50% (i.e., the box) of the forecast ensemble doesn't always embrace the observed outcome (red dot). Applying this kind of thinking to all the ensemble forecasts made for the 25 – 29 June time period, a simple contingency-matrix approach (Fig. 9, left side) can be designed to analyze the entire forecast dataset. The results thereof are summarized in a table (Fig. 9, right side), which shows the Percent Correct (PC), Critical Success Index (CSI), False Alarm Rate (FAR), Probability Of Detection (POD), and the Pierce Skill Score (PSS), respectively, for the 3-, 6-, and 9-h ensemble forecasts and focusing on fractional echo area coverage within a gridbox of 400 km. The forecast performance based on these numbers seems pretty good; however, we have to keep in mind that the forecast skill depends on the spatial scale of the analysis, an intensity threshold applied, and the type of weather present.

Additional analyses aimed at shedding light on a potential dependence of forecast skill on the magnitude of weather event are discussed next. This includes analyses of both weather and aviation-relevant information.

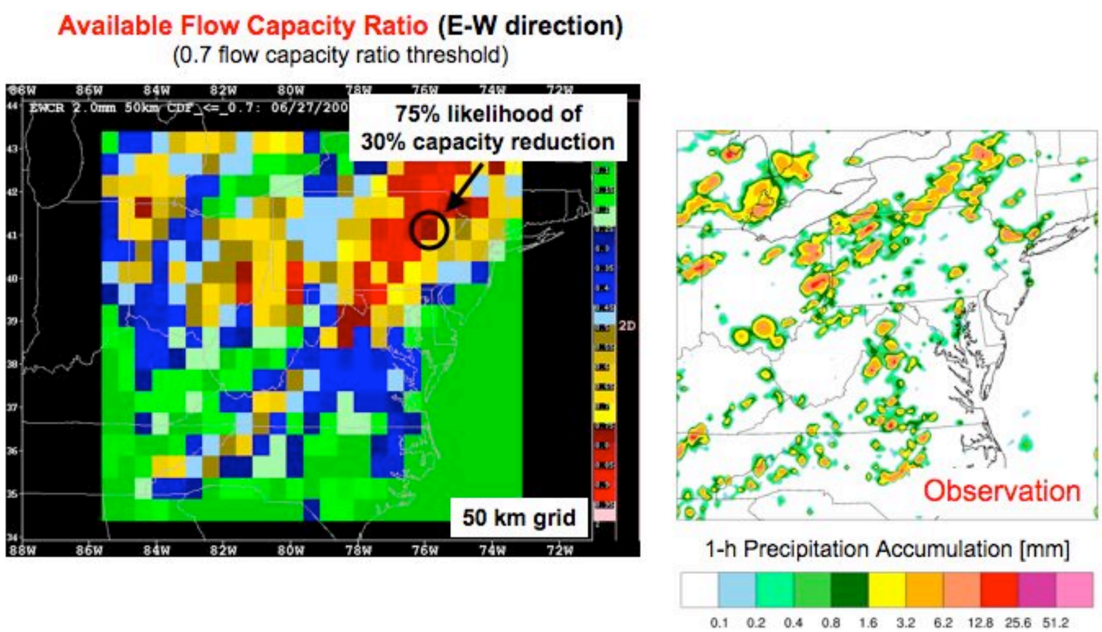

Figure 7. Predicted probabilistic available flow capacity ratio (left) based on expected weather hazards to be present on 27 June 2007 at 21 UTC versus observed actual weather (right).

3.2 Aviation focus

Figure 10 highlights a marked trend of the ensemble model forecast performance as a function of the magnitude of weather event. Each panel of Figure 10 shows the difference between modeled and observed parameter values based on all ensemble members for the available flow capacity ratio (upper panels) and the fractional echo area coverage (lower panels). The results based on the 3-h forecasts are shown in the left panels, the 6-h forecasts in the middle panels, and the 9-h forecasts in the right panels. Within each panel, all the values of difference between ensemble member and observation are grouped into several bins representing a magnitude range of the weather event. For example, the available flow capacity ratio is grouped into bins of values smaller than 0.5, 0.5 – 0.89, 0.9 – 0.99, and unity. Similarly, the fractional echo area coverage is divided into bins of 0% – 1%, 1% – 2%, 2% – 5%, and larger than 5%. For each bin, the distribution of values is visualized by a boxplot and the membership count is indicated at the bottom of the respective distribution.

At a 200-km gridbox scale, the ensemble model tends to increasingly overpredict the available flow capacity ratio with increasing magnitude of the weather event, as revealed by Figures 10a – 10c. This overprediction is directly related to a corresponding underprediction of the fractional echo area coverage, as shown by Figures 10d – 10f. Similar trends were observed for other spatial scales as well. A positive aspect of this behavior is that the observed trend seems to be essentially independent of the forecast lead time, which opens the door for a calibration by means of post-processing the data. A proper calibration, however, requires large amounts of data collected over long time periods, which remains to be done.

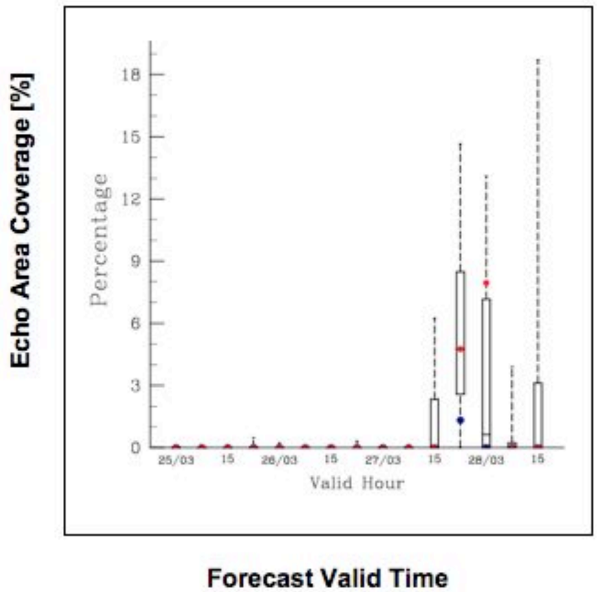

Figure 8. Timeseries of ensemble-based 9-h forecast spread of fractional echo area coverage for 25 – 29 June 2007 and one 400 km gridbox.

3.3 User impact

Assessment of ensemble-based probabilistic forecasts will not be complete without a proper evaluation of the forecast value to an aviation user. Plans are being made to utilize NASA's Future ATM Concepts Evaluation Tool (FACET) for a user impact evaluation.

4. SUMMARY

In the NextGen, air traffic management will be largely done by utilizing automated decision support tools that integrate probabilistic weather information. Toward developing that capability, this paper presented a concept of using ensemble-based numerical weather prediction model data for weather-related, probabilistic aviation impact forecasting. The approach combines: (1) the use of ensemble model data to create probabilistic information and (2) incorporation of the aviation user perspective directly into the analysis of ensemble data. The second aspect reflects a paradigm shift from "ensembling weather information" to "ensembling user-relevant information", which entails a translation of weather forecasts into aviation impact predictions.

This paper showed results of a proof of concept study that used convective storms as an example, but the approach is equally applicable to other aviation weather hazards, such as turbulence (already explored, but not discussed here), icing, or ceiling and visibility. It is envisioned that the proposed probabilistic, weather-related aviation impact forecasts will be used by air traffic controllers, traffic flow managers, and airline dispatchers to make strategic decisions on en route traffic flow as well as individual flights. However, it is also possible to tailor the presented concept for terminal area applications, such as predicting major wind shifts on runways, the onset of precipitation, or a transition from rain to snow at aviation-critical locations.

The results shown in this paper represent an initial assessment of the performance skill of probabilistic aviation impact predictions as a function of forecast lead-time, spatial scale, and magnitude of the impacting weather event. Additional work remains to be done, especially with regard to optimal creation of the ensemble membership and a proper calibration of the ensemble-based probabilistic forecasts—both of them constitute major modeling and verification community research efforts. Furthermore, the visualization of probabilistic aviation impact forecasts for human examination has to be optimized, the forecast products have to be evaluated under real-time conditions in an operational setting, and, last but not least, appropriate user training has to be implemented.

Acknowledgments. This work benefited in many ways from stimulating discussions with and assistance of Jimmy Krozel of Metron Aviation and William Chan of NASA Ames Research Center. The support provided by NASA under the MOA SAA2-402003 to NCAR is greatly appreciated.

REFERENCES

Betts, A. K., and M. J. Miller, 1986: A new convective adjustment scheme. Part II: Single column tests using GATE wave, BOMEX, ATEX and arctic air-mass data sets. *Quarterly Journal of the Royal Meteorological Society*, **112**(473), 693 – 709.

Chen, F., and J. Dudhia, 2001: Coupling an advanced land surface–hydrology model with the Penn State–NCAR MM5 modeling system. Part I: Model implementation and sensitivity. *Monthly Weather Review*, **129**(4), 569 – 585.

Chou, M.-D., and M. J. Suarez, 1994: *An Efficient Thermal Infrared Radiation Parameterization for Use in the General Circulation Models*. NASA Technical Memo NASA/TM-104604, 3, 92 pp.

Collins, W. D., P. J. Rasch, B. A. Boville, J. J. Hack, J. R. McCaa, D. L. Williamson, J. T. Kiehl, and B. Briegleb, 2004: *Description of the NCAR Community Atmosphere Model (CAM3.0)*. NCAR Technical Note, NCAR/TN-464+STR, 226 pp.

Dudhia, J., 1989: Numerical study of convection observed during the winter monsoon experiment using a mesoscale two-dimensional model. *Journal of the Atmospheric Sciences*, **46**(20), 3077 – 3107.

Gneiting, T., F. Balabdaoui, and A. E. Raftery, 2007: Probabilistic forecasts, calibration and sharpness. *Journal of the Royal Statistical Society Series B: Statistical Methodology*, **69**(2), 243 – 268.

Grell, G., 1993: Prognostic evaluation of assumptions used by cumulus parameterizations. *Monthly Weather Review*, **121**(3), 764 – 787.

Grell, G. A., and D. Dévényi, 2002: A generalized approach to parameterizing convection combining ensemble and data assimilation techniques. *Geophysical Research Letters*, **29**(14), 1693, doi:10.1029/2002GL015311, 4 pp.

Hong, S.-Y., and H.-L. Pan, 1996: Nonlocal boundary layer vertical diffusion in a medium-range forecast model. *Monthly Weather Review*, **124**(10), 2322 – 2339.

Hong, S.-Y., and J.-O. J. Lim, 2006: The WRF single-moment 6-class microphysics scheme (WSM6). *Journal of the Korean Meteorological Society*, **42**(2), 129 – 151.

Hong, S.-Y., H.-M. H. Juang, and Q. Zhao, 1998: Implementation of prognostic cloud scheme for a regional spectral model. *Monthly Weather Review*, **126**(10), 2621 – 2639.

Hong, S.-Y., Y. Noh, and J. Dudhia, 2006: A new vertical diffusion package with an explicit treatment of entrainment processes. *Monthly Weather Review*, **134**(9), 2318 – 2341.

Janjic, Z. I., 1994: The step-mountain eta coordinate model: Further developments of the convection, viscous sublayer and turbulence closure schemes. *Monthly Weather Review*, **122**(5), 927 – 945.

Janjic, Z. I., 2002: *Nonsingular implementation of the Mellor–Yamada level 2.5 scheme in the NCEP Meso model*. NCEP Office Note, No. 437, 61 pp.

Jones, M. S., B. A. Colle, and J. S. Tongue, 2007: Evaluation of a mesoscale short-range ensemble forecast system over the Northeast United States. *Weather and Forecasting*, **22**(1), 36 – 55.

Kain, J. S., and J. M. Fritsch, 1993: Convective parameterization for mesoscale models: The Kain–Fritsch scheme. *The Representation of Cumulus Convection in Numerical Models*, K. A. Emanuel and D. J. Raymond, Editors, American Meteorological Society, 246 pp.

Krozel, J., J. S. B. Mitchell, V. Polishchuk, and J. Prete, 2007: Maximum flow rates for capacity estimation in level flight with convective weather constraints. *Air Traffic Control Quarterly*, **15**(3), 209 – 238.

Lin, Y.-L., R. D. Farley, and H. D. Orville, 1983: Bulk parameterization of the snow field in a cloud model. *Journal of Climate and Applied Meteorology*, **22**(6), 1065 – 1092.

Liu, Y., F. Chen, T. Warner, and J. Basara, 2006: Verification of a mesoscale data-assimilation and forecasting system for the Oklahoma City area during the Joint Urban 2003 Field Project. *Journal of Applied Meteorology and Climatology*, **45**(7), 912 – 929.

Liu, Y., M. Xu, J. Hacker, T. Warner, and S. Swerdlin, 2007: A WRF and MM5-based 4-D mesoscale ensemble data analysis and prediction system (E-RTFDDA) developed for ATEC operational applications. *22nd Conference on Weather Analysis and Forecasting and 18th Conference on Numerical Weather Prediction*, Park City, UT, American Meteorological Society, Paper 7B.7, 8 pp.

Liu, Y., T. T. Warner, J. F. Bowers, L. P. Carson, F. Chen, C. A. Clough, C. A. Davis, C. H. Egeland, S. F. Halvorson, T. W. Huck Jr., L. Lachapelle, R. E. Malone, D. L. Rife, R.-S. Sheu, S. P. Swerdlin, and D. S. Weingarten, 2008: The operational mesogamma-scale analysis and forecast system of the U.S. Army Test and Evaluation Command. Part I: Overview of the modeling system, the forecast products, and how the products are used. *Journal of Applied Meteorology and Climatology*, **47**(4), 1077 – 1092.

Mitchell, J. S. B., V. Polishchuk, and J. Krozel, 2006: Airspace throughput analysis considering stochastic weather. *AIAA Guidance, Navigation, and Control Conference*, Keystone, CO, August, 19 pp.

Mlawer, E. J., S. J. Taubman, P. D. Brown, M. J. Iacono, and S. A. Clough, 1997: Radiative transfer for inhomogeneous atmospheres:RRTM, a validated correlated-k model for the longwave. *Journal of Geophysical Research*, **102**(D14), 16663 – 16682.

Reisner, J., R. M. Rasmussen, and R. T. Bruintjes, 1998: Explicit forecasting of supercooled liquid water in winter storms using the MM5 mesoscale model. *Quarterly Journal of the Royal Meteorological Society*, **124B**(548), 1071 – 1107.

Rogers, E., T. Black, B. Ferrier, Y. Lin, D. Parrish, and G. DiMego, 2001: *Changes to the NCEP Meso Eta Analysis and Forecast System: Increase in Resolution, new Cloud Microphysics, modified Precipitation Assimilation, modified 3DVAR Analysis*. NOAA Technical Procedures Bulletin (TPB), online accessible at http://www.emc.ncep.noaa.gov/mmb/mmbpll/eta12tpb/

Schwarzkopf, M. D., and S. B. Fels, 1991: The simplified exchange method revisited: An accurate, rapid method for computation of infrared cooling rates and fluxes. *Journal of Geophysical Research*, **95**(D5), 9075 – 9096.

Song, L., C. Wanke, D. P. Greenbaum, and D. A. Callner, 2007: Predicting sector capacity under severe weather impact for traffic flow management. *7th AIAA Aviation Technology, Integration and Operations Conference*, Belfast, Northern Ireland, September, AIAA 2007-7887, 12 pp.

Song, L., C. Wanke, D. Greenbaum, S. Zobell, and C. Jackson, 2008: Methodologies for estimating the impact of severe weather on airspace capacity. *8th AIAA Aviation Technology, Integration and Operations Conference*, Anchorage, AK, September, AIAA 2008-8917, 12 pp.

Steiner, M., C. K. Mueller, G. Davidson, and J. A. Krozel, 2008: Integration of probabilistic weather information with air traffic management decision support tools: A conceptual vision for the future. *13th Conference on Aviation, Range and Aerospace Meteorology*, Amer. Meteor. Soc., New Orleans, LA, 4.1, 9 pp.

Stensrud, D. J., and N. Yussouf, 2007: Reliable probabilistic quantitative precipitation forecasts from a short-range ensemble forecasting system. *Weather and Forecasting*, **22**(1), 3 – 17.

Tao, W.-K., and J. Simpson, 1993: Goddard cumulus ensemble model. Part I: Model description. *Terrestrial, Atmospheric and Oceanic Sciences*, **4**(1), 35 – 72.

Thompson, G., P. R. Field, W. D. Hall, and R. M. Rasmussen, 2006: A new bulk microphysical parameterization in WRF. *7th WRF and 16th MM5 Users' Workshop*, NCAR, Boulder, CO, June, 11 pp.

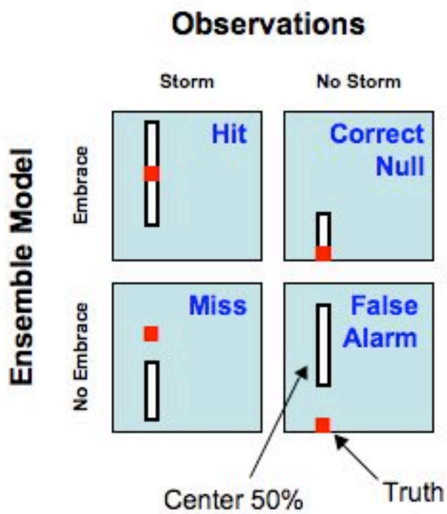

	3 h	6 h	9 h
PC	0.85	0.83	0.81
CSI	0.55	0.47	0.47
FAR	0.06	0.07	0.00
POD	0.59	0.50	0.47
PSS	0.56	0.47	0.47

Figure 9. Forecast performance skill assessment design and summary statistics for 25 – 29 June 2007 and 400 km gridboxes.

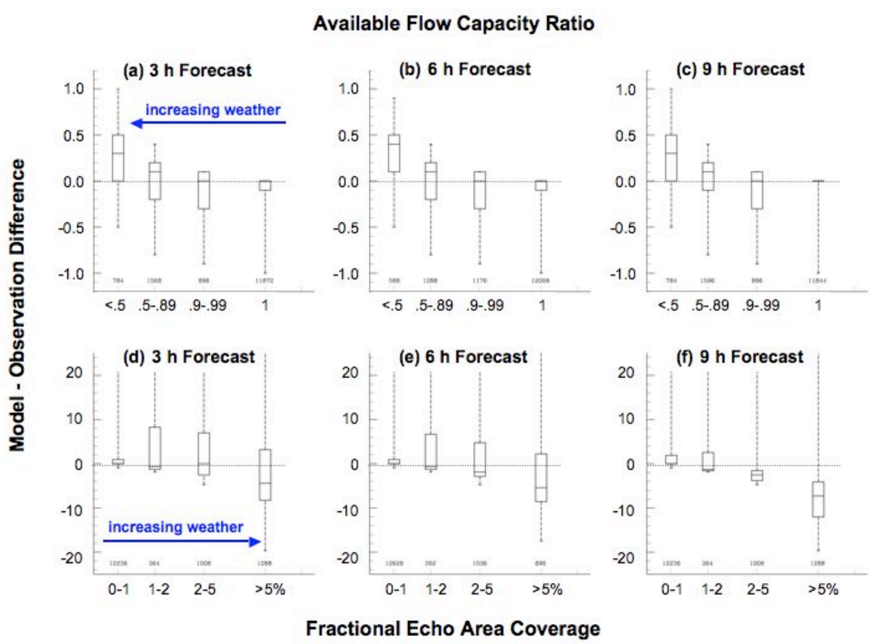

Figure 10. Ensemble prediction performance assessment of the available flow capacity ratio (upper panels) and fractional echo area coverage (lower panels) based on corresponding observations and magnitude of weather constraints for 200 km gridboxes and RNP = 4.

Table 1. Overview of the ensemble RT-FDDA membership configuration. The control runs ("CTRL") are indicated by the gray shading. For the other ensemble members only the respective modification (compared to the control run) is pointed out. [CPS = Convective Parameterization Scheme; MPS = MicroPhysics Scheme; PBL = Planetary Boundary Layer; LSS = Land Surface Scheme; LRS = Longwave Radiation Scheme; SRS = Shortwave Radiation Scheme.]

Model	Initialization	Configuration	Label
MM5	GFS	CPS: Grell (1993) MPS: Reisner et al. (1998) PBL: Hong and Pan (1996) LSS: Chen and Dudhia (2001) LRS: Mlawer et al. (1997) SRS: Dudhia (1989)	GFS-M-CTRL
		Same as GFS-M-CTRL, except alternate CPS: Betts and Miller (1986)	GFS-M-CBM1
		Same as GFS-M-CTRL, except alternate CPS: Kain and Fritsch (1993)	GFS-M-CKF2
		Same as GFS-M-CTRL, except alternate MPS: Tao and Simpson (1993)	GFS-M-MGOD
		Same as GFS-M-CTRL, except alternate MPS: Reisner et al. (1998), with graupel	GFS-M-MRE2
		Same as GFS-M-CTRL, except random positive perturbation of surface observations	GFS-M-SFCA
		Same as GFS-M-CTRL, except random negative perturbation of surface observations	GFS-M-SFCB
	NAM	Same as GFS-M-CTRL, except for different initialization	NAM-M-CTRL
		Same as NAM-M-CTRL, except alternate CPS: Betts and Miller (1986)	NAM-M-CBM1
		Same as NAM-M-CTRL, except alternate CPS: Kain and Fritsch (1993)	NAM-M-CKF2
		Same as NAM-M-CTRL, except alternate MP: Tao and Simpson (1993)	NAM-M-MGOD
		Same as NAM-M-CTRL, except alternate MP: Reisner et al. (1998), with graupel	NAM-M-MRE2
		Same as NAM-M-CTRL, except reduced radius of influence for observation nudging	NAM-M-R100
		Same as NAM-M-CTRL, except random positive perturbation of upper air observations	NAM-M-UPRA
		Same as NAM-M-CTRL, except random negative perturbation of upper air observations	NAM-M-UPRB

Table 1. (continued)

Model	Initialization	Configuration	Label
WRF	GFS	CPS: Kain and Fritsch (1993), modified MPS: Lin et al. (1983) PBL: Hong et al. (2006) LSS: Chen and Dudhia (2001) LRS: Mlawer et al. (1997) SRS: Dudhia (1989)	GFS-W-CTRL
		Same as GFS-W-CTRL, except alternate CPS: Janjic (1994)	GFS-W-CBMJ
		Same as GFS-W-CTRL, except alternate CPS: Grell and Dévényi (2002)	GFS-W-CGDE
		Same as GFS-W-CTRL, except alternate MPS: Rogers et al. (2001)	GFS-W-MFER
		Same as GFS-W-CTRL, except alternate MPS: Thompson et al. (2006)	GFS-W-MTHO
		Same as GFS-W-CTRL, except alternate MPS: Hong and Lim (2006)	GFS-W-MWS6
		Same as GFS-W-CTRL, except alternate PBL: Janjic (2002)	GFS-W-PMYJ
		Same as GFS-W-CTRL, except alternate LRS&SRS: Collins et al. (2004)	GFS-W-RCAM
		Same as GFS-W-CTRL, except alternate LRS: Schwarzkopf and Fels (1991)	GFS-W-RGFD
		Same as GFS-W-CTRL, except alternate SRS: Chou and Suarez (1994)	GFS-W-RGOD
	NAM	Same as GFS-W-CTRL, except for different initialization	NAM-W-CTRL
		Same as NAM-W-CTRL, except alternate MPS: Hong et al. (1998)	NAM-W-MWS5
		Same as NAM-W-CTRL, except alternate PBL: Janjic (2002)	NAM-W-PMYJ